Raman-scattering study of the Li^+ and $F_A(Li^+)$ centers in KBr

Marc Leblans, Wim Joosen, and Dirk Schoemaker
Department of Physics, University of Antwerp (Universitaire Instelling Antwerpen), Universiteitsplein 1, B-2610 Wilrijk (Antwerp), Belgium

Abdul Mabud and Fritz Lüty
Department of Physics, University of Utah, Salt Lake City, Utah 84112
(Received 1 September 1988)

It was recently shown for the $F_A(Li^+)$ center in KCl:Li^+ that polarized resonant Raman scattering spectra analyzed with the Zhou-Goovaerts-Schoemaker behavior-type (BT) method [Phys. Rev. B **29**, 5509 (1984)] allow one to establish the off-center position of the Li^+ impurity ion in this center. The present study reports the resonant Raman spectra of $F_A(^7Li^+)$ and $F_A(^6Li^+)$ in KBr. The BT analysis of the polarized Raman data establishes a C_{4v} defect symmetry indicating the on-center position of the Li^+ ion in this defect, in agreement with the on-site location of the isolated Li^+ ion in KBr. Among the many observed modes, $F_A(Li^+)$ in KBr possesses a vibrational mode at 227 cm^{-1}, which reflects the motion of Li^+ along the fourfold defect axis, as indicated by its regular isotope effect. Its vibrational energy strongly exceeds that of the 17-cm^{-1} infrared mode of the isolated Li^+ ion, demonstrating that the adjacent electron in the $F_A(Li^+)$ center strongly disturbs the potential experienced by the Li^+ ion. A mode at 28 cm^{-1} also associated with the Li^+ impurity exclusively appears under F_{A1} excitation and shows by the absence of an isotope effect very small participation of Li^+ motion. The other dynamical modes of KBr:$F_A(Li^+)$ are defect-induced lattice modes with peak positions close to those of the unperturbed F center. However, they possess different relative peak heights and polarized Raman intensities. A comparison with the vibrations of the $F_A(Li^+)$ center in KCl is presented and the low-frequency Raman- and infrared-active modes of the isolated Li^+ impurity in KBr are also reported. It is suggested that both static and dynamic anharmonicities are important for the description of these low-frequency modes.

I. INTRODUCTION

The off- or on-center position of the substitutional Li^+ ion in KBr has been a controversial subject both from a theoretical and an experimental viewpoint. One reason for this was the lack of a precise identification of the Li^+ center under study.[1] By means of paraelectric resonance and far-infrared- (ir-) absorption measurements it was recently recognized that at least two different Li^+ centers occur in the KBr host. The first is a nontunneling isolated Li^+ impurity ion, for which no paraelectricity was observed. This defect gives rise to an ir-active mode at about 17 cm^{-1}. The second is a relatively-low-concentration Li^+-pair center, which exhibits a peculiar paraelectric behavior and a tunneling motion, both of which are still not yet well understood.[1-3]

The present Raman-scattering study focuses on the dynamics of the isolated substitutional Li^+ ion. Extensive experimental data (summarized in Ref. 1) indicate that the Li^+ ion in KBr is located on center. However, theoretical predictions concerning the off- or on-center position were contradictory, since the existence and the location of off-center potential minima is extremely sensitive to the parameters of the repulsive part of the potential.[4-7] It is still an intriguing problem to characterize the Li^+ potential in KBr to such an extent that it describes the Li^+ dynamical modes, as studied from far-ir and Raman measurements. From this perspective a comparison between KBr:Li^+ and KCl:Li^+ is very interesting. In KCl the Li^+ ion is definitely located *off-center*, yielding typical paraelectric and paraelastic behavior. In contrast, KBr:Li^+, being a borderline case for off-center versus on-center behavior, exhibits peculiar dynamical properties, which cannot be straightforwardly explained.

The isolated Li^+ ion in KBr exhibits low-frequency ir- and Raman-active modes.[8,9] A summary and brief description of these dynamical modes will be given in Sec. III. The $F_A(Li^+)$ center has only been studied with the Raman-scattering technique and first results have been presented in Ref. 10. It possesses defect-induced phonon modes, often with several observable overtones or combination bands above the cutoff frequency, which are similar to the pure F-center-induced lattice modes. In KCl the vibrations above the cutoff frequency are undoubtedly associated with motions of the Li^+ impurity itself.[11-14] This is not so obvious for the $F_A(Li^+)$ center in KBr. We will compare the vibrational modes of KCl:Li^+ and KCl:$F_A(Li^+)$ to those of KBr:Li^+ and KBr:$F_A(Li^+)$, respectively, since the observability and the properties of these modes reflect details of the different impurity potentials in the two hosts.

The $F_A(Li^+)$ center in KBr provides another interest-

ing test case for the Zhou-Goovaerts-Schoemaker behavior-type (BT) analysis of polarized Raman data.[14–16] With this method it was possible to determine the off-center position of Li^+ in the KCl:$F_A(Li^+)$ system, based on the polarized Raman data only.[14] A similar Raman study of the KBr:$F_A(Li^+)$ system should be illuminating, especially in view of the controversial results obtained earlier for the KBr:Li^+ defect system.

The outline of this paper is the following. Experimental details are given in Sec. II. Sec. III contains a description of the experimentally observed dynamical modes of the Li^+ and $F_A(Li^+)$ centers in KBr and KCl. The properties of the low-frequency Raman and ir modes of Li^+ are summarized and the resonant Raman-scattering spectra of the corresponding $F_A(Li^+)$ centers are also reported. The data are interpreted in Sec. IV. The polarized Raman spectra are correlated to the defect symmetry and the location of the Li^+ ion. The nature of the dynamical modes of $F_A(Li^+)$ is discussed as well as their coupling to the F_{A1} and F_{A2} transitions. The main conclusions and some remaining problems are pointed out in Sec. V.

II. EXPERIMENTAL DETAILS

The crystals used for this investigation were grown at the University of Utah (Salt Lake City) and Paderborn University (West Germany) laboratories, and at ENEA [Centro Ricerche Energia Frascati (Italy)]. The Raman data were taken on additively colored crystals at Utah and on x-irradiated KBr:Li^+ crystals at the University of Antwerp. While in the first samples nearly complete $F \rightarrow F_A$ conversion is possible, in the latter samples the relative concentration of the F_A centers with respect to the F centers is comparatively lower, because the conversion to F_A centers is never complete. This encumbers the interpretation of some of the polarized Raman data, particularly those obtained under resonant excitation of the F_{A2} transition, which is nearly coincident with the F band. Samples with natural (93% $^7Li^+$) abundance and with enriched concentration of $^6Li^+$ isotopes were studied. About 1 mol% of lithium halide was added to the melt. The resonant Raman spectra of the $F_A(Li^+)$ center were recorded at 10 K, excited with a Kr^+-ion laser (568, 647, and 676 nm) or a He-Ne laser (632 nm).

III. RAMAN AND INFRARED SPECTRA OF Li^+ AND $F_A(Li^+)$ IN KBr

A. Low-frequency modes of the isolated Li^+ center in KBr

The $^7Li^+$ ion in KBr exhibits a far-ir resonant mode at 16.3 cm^{-1} with an absorption constant of about 12 cm^{-1} for an impurity concentration of $1.3\times10^{18}/cm^3$. The peak position shifts to 17.9 cm^{-1} upon $^7Li^+$-to-$^6Li^+$ substitution. The size of this isotope effect (ratio 1.10) slightly exceeds that of an Einstein oscillator (ratio 1.08). The ir spectra also show weaker impurity modes at 43 and 45 cm^{-1} for $^7Li^+$ and $^6Li^+$, respectively, which are possibly the second overtones of the low-frequency resonance, as was suggested in Ref. 8.

In addition to the odd-parity (T_{1u}) ir vibration, the KBr:Li^+ defect also possesses two low-frequency *Raman*-active transitions at 37 and 27 cm^{-1} for $^7Li^+$. Although these transitions are even with respect to the Li^+ lattice site, they do exhibit an isotope effect[9] with ratio 1.09 and 1.08 for the 37- and 28-cm^{-1} modes, respectively. The polarized Raman measurements established that these modes transform according to the A_{1g} and the E_g representations (in that order) of the cubic group. No T_{2g} contribution was observed.[9]

B. Resonant Raman spectra of $F_A(Li^+)$ in KBr

1. $F_A(Li^+)$-induced lattice modes

Below the phonon cutoff frequency at 166 cm^{-1} the $F_A(Li^+)$ spectrum in KBr consists of a continuum of defect-induced acoustic- and optical-phonon modes. The sharp peaks at 97, 106, and 119 cm^{-1} closely resemble those of the unperturbed F center in KBr, since they possess approximately the same Raman shift (Fig. 1). The

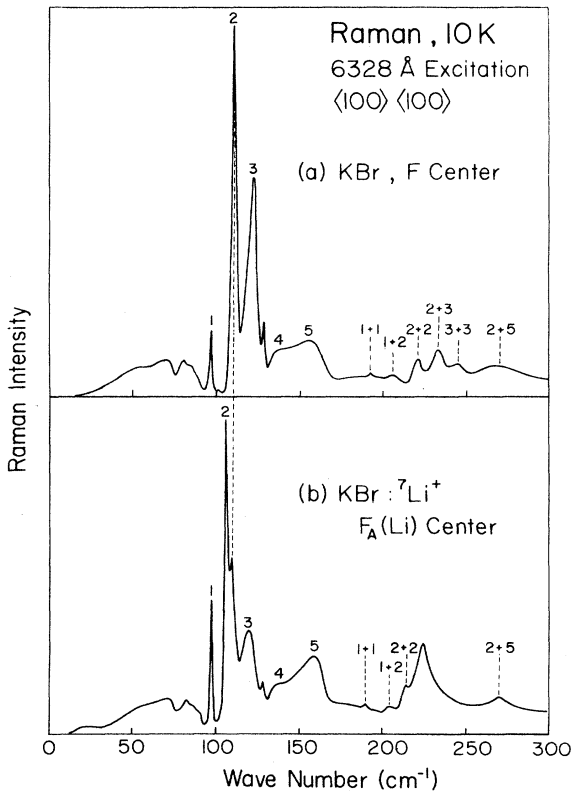

FIG. 1. (a) Resonant Raman spectrum of the F center in an additively colored KBr sample. The most prominent F-center-induced phonons, together with their overtones and combination bands, are labeled with numbers. (b) F_A center spectrum in an additively colored KBr: $^7Li^+$ sample. The phonon mode (2) has a different spectral position in (a) and (b) and is useful to monitor the F-to-F_A conversion. Note the Li^+-induced modes at 28 and 227 cm^{-1} in (b).

peak positions of the most prominent "common" spectral features of the F and F_A center are listed in Table I. Above the phonon cutoff several overtones and combination bands of these fundamental modes are detected (Fig. 1). Their spectral positions are listed in Table I. A comparison between the F- and the F_A-center spectra shows that the additional vibrational modes in the $F_A(Li^+)$ spectrum at 28 and 227 cm^{-1} are associated with the Li^+ impurity.

2. *The 28- and 227-cm^{-1} Raman modes: Isotope effects*

In KBr:$F_A(^7Li^+)$ we observed two dynamical modes at 28 and 227 cm^{-1}, which are specific for the Li^+ impurity in the sense that there is no corresponding F-center vibration. The high-frequency mode exhibits an isotope shift to 243 cm^{-1} upon $^7Li^+$-to-$^6Li^+$ substitution, which clearly correlates it with a motion of the Li^+ ion itself.[10] This isotope effect is shown in Fig. 2. The KBr:$F_A(^6Li^+)$ spectrum is of crucial importance for the identification of this Li^+ high-frequency mode. On one hand, its vibrational energy is nearly degenerate with the sum frequency of the 106- and 119-cm^{-1} modes and the polarized Raman properties are similar to those of the $F_A(Li^+)$-induced lattice modes (see Fig. 3 and Table II in the next subsection). This may lead one into thinking that one is dealing with a combination mode. However, the Raman spectrum in Fig. 2 clearly shows the $^6Li^+$ vibration at 243 cm^{-1}, well separated from the combination band at about 225 cm^{-1}.

Within experimental accuracy the low-frequency vibration at 28 cm^{-1} does not exhibit an isotope shift upon $^7Li^+$-to-$^6Li^+$ substitution. Surprisingly, it shows up only under F_{A1} excitation. For the isolated Li^+ center in KBr, no dynamical mode corresponding to this 28-cm^{-1} vibration has been observed, either in far-ir absorption or in Raman scattering. Such a Raman mode would be superimposed on the E_g mode at 27 cm^{-1}, from which it could be distinguished by its polarization properties.

TABLE I. Dynamical modes of the F center and the $F_A(^7Li^+)$ center in KBr. The vibrational energies are given in wave numbers. The modes above the phonon cutoff frequency are identified as overtones or combination bands of the fundamental transitions ν_1, ν_2, ν_3, ν_4, and ν_5.

KBr:F (cm^{-1})	KBr:$F_A(Li^+)$ (cm^{-1})	Identification
97	97	ν_1
112	106	ν_2
123	119	ν_3
~135	~135	ν_4
~160	~160	ν_5
193	193	$2\nu_1$
208	204	$\nu_1+\nu_2$
223	213	$2\nu_2$
233	225[a]	$\nu_2+\nu_3$
245		$2\nu_3$
~270	~270	$\nu_2+\nu_5$

[a]Nearly degenerate with the Li^+ vibration.

3. *Polarized Raman spectra under F_{A1} and F_{A2} excitation*

The frequency dependence of the polarized Raman spectra is shown in Fig. 3 for resonant excitation in the F_{A1} (676- and 647-nm) and F_{A2} (568-nm) bands. The data are indicated by $\langle\alpha\rangle\langle\beta\rangle$, in which α and β (in that order) are the polarization vectors of the incident and scattered light in the crystal reference frame. The spectrum observed under 568-nm excitation still contains a considerable F-center contribution, as is reflected in the asymmetric shape and the spectral position of the highest peak in the $\langle 110\rangle\langle 110\rangle$ spectrum. According to the relative intensities of the sharp peaks at 112 and 106 cm^{-1} under 568- and 632-nm excitation, the F_A-center contribution to the F_{A2} spectrum (568 nm) is estimated to be about 50%. The polarized Raman properties of the $F_A(Li^+)$ center under F_{A2} excitation closely resemble those of the isolated F center: the dominant contribution

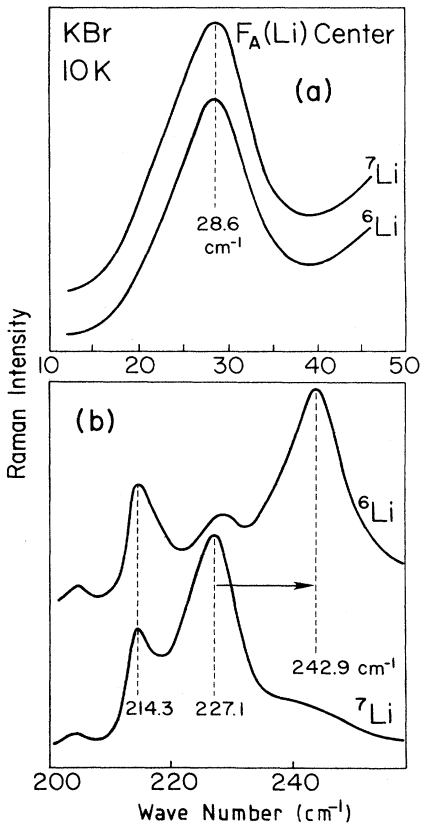

FIG. 2. Isotope effect of the $F_A(Li^+)$ modes in additively colored KBr at 28 and 227 cm^{-1} upon $^7Li^+$-to-$^6Li^+$ substitution under F_{A1} excitation. The low-frequency mode at 28 cm^{-1} does not exhibit an isotope effect (a), while the 227-cm^{-1} mode shifts up to 243 cm^{-1} (b). Note the combination band at about 227 cm^{-1} [mode (2+3) in Fig. 1], which is nearly degenerate with the $F_A(^7Li^+)$ high-frequency vibration.

appears in the ⟨110⟩⟨110⟩ spectrum.[13] The depolarized Raman scattering, i.e., the ⟨110⟩⟨001⟩ spectrum, is comparatively weak. In particular, it is negligible for the 227-cm^{-1} mode of the $F_A(Li^+)$ center. The low-frequency mode at 28 cm^{-1} is not observed under F_{A2} excitation.

For F_{A1} excitation at 647 and 676 nm the polarized Raman intensities are very different. First, the 28-cm^{-1} mode is observed to exhibit zero depolarized scattering and equal intensities for the ⟨110⟩⟨110⟩ and ⟨1$\bar{1}$0⟩⟨110⟩ spectra. Apart from the acoustic and optical phonons the depolarized scattering is negligibly small for all modes. This is, in particular, the case for the sharp peaks at 97, 106, and 119 cm^{-1} (labeled 1, 2, and 3 in Fig. 1), their overtones and combination bands, and for the Li^+ mode at 227 cm^{-1}. The fact that the ⟨1$\bar{1}$0⟩⟨110⟩ contribution is more intense than the ⟨110⟩⟨110⟩ spectrum is very specific for the $F_A(Li^+)$ center in KBr and will be discussed in Sec. IV.

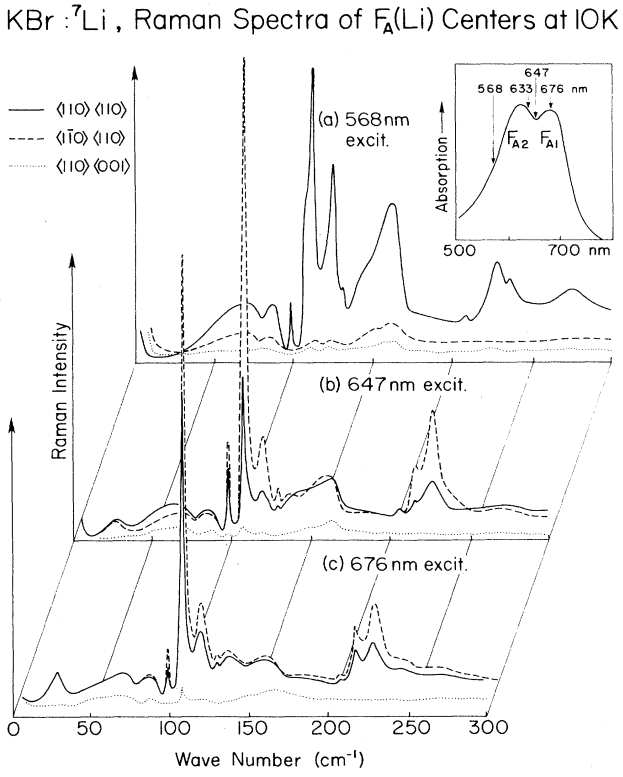

FIG. 3. Frequency dependence of the polarized Raman spectra in additively colored KBr:$F_A(^7Li)$ under F_{A1} and F_{A2} excitation, as indicated in the inset. The 568-nm spectrum still contains a contribution of isolated F centers. Under excitation at longer wavelengths, the $F_A(Li^+)$ features become dominant, i.e., the Li^+-induced modes at 28 and 227 cm^{-1}, and the $F_A(Li^+)$-induced phonon mode at 106 cm^{-1}. The polarized Raman properties are very different under F_{A1} and F_{A2} excitation, as is reflected in the relative intensities of the ⟨110⟩⟨110⟩ and ⟨1$\bar{1}$0⟩⟨110⟩ spectra.

4. *Behavior-type analysis of the polarized Raman data*

For the present discussion we assume that the $F_A(Li^+)$ centers are randomly distributed among their possible orientations. This assumption does not influence the conclusions of the BT analysis, as will be discussed in the Appendix. In Fig. 4 a set of polarized Raman data $I_{\alpha,\beta}$ is presented, together with the essential information on the observed BT.[15] The Raman intensities are expressed in terms of the intensity parameters (IP's)[15] s, q, and r:

$$s = kI_0N(T_{12}^2 + T_{23}^2 + T_{31}^2) , \tag{1a}$$

$$q = kI_0N(T_{11}^2 + T_{22}^2 + T_{33}^2) , \tag{1b}$$

$$r = kI_0N(T_{11}T_{22} + T_{22}T_{33} + T_{33}T_{11}) . \tag{1c}$$

The T_{ij} are the components of the Raman tensor for an arbitrary initial orientation of the defect, expressed in the crystal reference frame. N is proportional to the defect concentration, k is the instrumental efficiency, and I_0 is the intensity of the incident laser light. The IP's q, r, and s can be determined from the data $I_{\alpha,\beta}$ and their relative values are also indicated in Fig. 4. All information about the symmetry-related properties of the Raman tensor and the populations numbers is contained in the ratios s/q and r/q. They are listed in Table II for some specific vibrational modes of $F_A(Li^+)$ in KBr.

The acoustic and optical band modes possess F-center-like polarized Raman properties and do not reflect deviations from the cubic symmetry. For the determination of

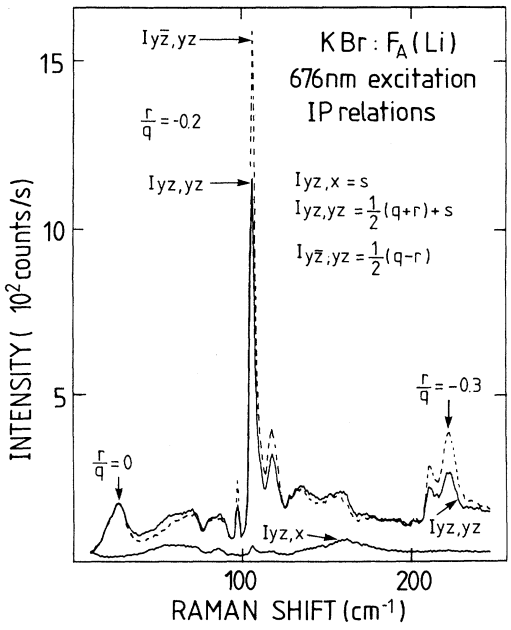

FIG. 4. Polarized Raman spectra under 676-nm excitation in a KBr:$^7Li^+$ sample, which was x irradiated for 20 min and subsequently $F \rightarrow F_A$ converted by bleaching in the F band. The polarized Raman spectra are expressed in terms of the intensity parameters q, r, and s, which are used in the behavior-type analysis.

TABLE II. Relative polarized Raman intensities s/q and r/q under F_{A1} and F_{A2} excitation for some typical $F_A(^7Li^+)$ vibrations. The Raman shifts are given in wave numbers (cm^{-1}).

$F_A(Li^+)$ mode (cm^{-1})	s/q 568 nm	s/q 647 nm	s/q 676 nm	r/q 568 nm	r/q 647 nm	r/q 676 nm
28		0.00±0.05	0.00±0.05		0.00±0.05	0.00±0.05
107	0.05±0.03	0.00±0.02	0.00±0.02	0.9±0.1	−0.50±0.05	−0.20±0.05
165	0.09±0.03	0.3±0.1	0.2±0.1	0.6±0.1	−0.2±0.1	−0.07±0.10
227	0.0±0.1	0.00±0.05	0.00±0.02	1.0±0.1	−0.50±0.05	−0.30±0.05

the defect symmetry from the polarized Raman data we concentrate on the $F_A(Li^+)$ modes at 28 and 227 cm^{-1}, and on the sharp peaks at 97, 106, and 119 cm^{-1}. The s/q ratio of all these Raman modes is equal to zero, within experimental error. The r/q ratio is zero for the 28-cm^{-1} mode and negative for the other $F_A(Li^+)$ vibrations. These two IP relations define the BT no. 50 (Ref. 15), which is consistent with the C_{4v} point group.[14] The negative r/q ratio is discussed in Sec. IV.

C. Comparison with KCl:Li^+ and KCl:$F_A(Li^+)$ Raman and infrared spectra

The isolated Li^+ off-center impurity in KCl possesses a low-frequency vibrational mode at 43 cm^{-1}, which is both ir[17] and Raman active.[9,18] The intensity of the KCl:Li^+ ir mode is weaker than that in KBr:Li^+: for a Li^+ impurity concentration of $2.3\times10^{18}/cm^3$ in KCl the absorption constant is typically 4 cm^{-1}. In KCl:Li^+ the low-frequency vibration has both in ir and Raman a small and anomalous isotope effect,[9,17] indicating that the Li^+ coordinate is hardly involved in this dynamical mode. Consequently, this ir mode derives from an even-parity (A_{1g}) vibration and its observability is due to the off-center relaxation of Li^+ in KCl. Its isotope shift[9,17] may probably originate from the coupling to the tunneling motion of Li^+ (Ref. 19). The low-frequency Raman and ir modes of the isolated Li^+ centers in KCl and KBr are summarized in Table III.

The low-frequency ir mode at 16.3 cm^{-1} in KBr:Li^+ reflects the $^7Li^+$ motion through its observed normal isotope effect, and does not possess a Raman-active mode of similar frequency. Moreover, the Raman transitions with normal isotope effect, i.e., those at 27 and 37 cm^{-1}, are not directly correlated with the vibrational energy of the low-frequency ir mode (see Table III). For both the KCl:Li^+ and KBr:Li^+ systems no high-frequency modes were observed either in Raman scattering or in ir absorption, although a theoretical calculation for KCl:Li^+ predicted Li^+ vibrations at 280 and 380 cm^{-1}.[20]

The resonant Raman spectra of $F_A(Li^+)$ in KCl and KBr exhibit high-frequency modes with a normal Li^+ isotope shift for excitation in the F_{A1} and F_{A2} bands. Only under F_{A1} excitation is a low-frequency vibration detected at 47 and 28 cm^{-1} in KCl and KBr, respectively. In KCl the properties of this $F_A(Li^+)$ mode are similar to those of the low-frequency mode of the isolated Li^+ center. This is in contrast with KBr, in which the low-frequency modes of the isolated Li^+ ion and the $F_A(Li^+)$ center exhibit different polarized Raman properties, isotope effects, and vibrational energies.

TABLE III. The low-frequency vibrations of the isolated Li^+ centers in KCl and KBr are given for both Li^+ isotopes. For KBr:Li^+ the ir spectrum contains the fundamental modes and the second overtones (SO), while the first overtones (FO) show up in the Raman spectrum. The KCl:Li^+ mode is both Raman and ir active. Peak positions are given in wave numbers.

Center	Infrared	Infrared	Raman
KCl:$^6Li^+$	39.5[a]		43[c]
KCl:$^7Li^+$	42.1[a]		44[d]
KBr:$^6Li^+$	17.9[b]	45.5 (SO)[b]	28,40 (FO)[c]
KBr:$^7Li^+$	16.3[b]	43.0 (SO)[b]	27,37 (FO)[c]

[a]Reference 17.
[b]Reference 8.
[c]Reference 9.
[d]References 9 and 18.

IV. DYNAMICS OF THE Li^+ AND $F_A(Li^+)$ CENTERS IN KBr

A. The on-center position of the Li^+ ion in KBr:$F_A(Li^+)$

The Li^+ ion in KBr:$F_A(Li^+)$ can be located on or away from the C_{4v} axis of the center. The corresponding defect symmetry is reflected in the form of the Raman tensor of the vibrational modes of the $F_A(Li^+)$ center. We have established BT no. 50 for the $F_A(Li^+)$ vibrations at 28, 97, 106, 119, and 227 cm^{-1} through the observation of the zero s/q ratio. In earlier work we observed the same quantitative behavior for the polarized Raman intensities of some particular dynamical modes of the $F_A(Li^+)$ center in KCl, the Tl^+-perturbed $Tl^0(1)$ center, and the unperturbed $Tl^0(1)$ center.[14,16,21] According to the BT analysis it is concluded that these $F_A(Li^+)$ modes transform like the A_1 representation of the C_{4v} point group. This defect symmetry corresponds to an on-center position of the Li^+ ion in the $F_A(Li^+)$ defect in KBr.

B. Coupling of the $F_A(Li^+)$ vibrations with the F_{A1} and F_{A2} transitions

Earlier Raman work on the laser-active $Tl^0(1)$ center,[21] the $F_A(Li^+)$ center in KCl,[14] and the Tl^+-perturbed

$Tl^0(1)$ defect in KCl, KBr, and RbCl (Ref. 16) has shown that resonant enhancement (RE) of particular components of the Raman tensor, i.e., *selective* RE (SRE), can strongly influence the IP ratios and may even obscure the actual defect symmetry. This is clearly illustrated by the 216-cm^{-1} mode of the $F_A(Li^+)$ center in KCl: Under F_{A2} excitation, its s/q ratio reflects the off-center position of the Li^+ ion, which is not the case under F_{A1} excitation. For the $F_A(Li^+)$ modes in KBr the s/q ratio is equal to zero *both* under F_{A1} and F_{A2} excitation, which is consistent with the C_{4v} point group of this center.

The r/q ratio of the $F_A(Li^+)$ modes in KBr (i) clearly depends on the nature of the dynamical mode, (ii) is strongly frequency dependent, (iii) is negative for several modes under 647- and 676-nm (F_{A1}) excitation, and (iv) possesses a magnitude ranging from zero for the 28-cm^{-1} mode under F_{A1} excitation to about unity for the 227-cm^{-1} mode under F_{A2} excitation. These four features will now be discussed in some detail.

(i) According to the BT analysis all the $F_A(Li^+)$ vibrations transform according to the A_1 representation of C_{4v}. Its Raman tensor is

$$C_{4v}:\ A_1 \begin{bmatrix} a & 0 & 0 \\ 0 & a & 0 \\ 0 & 0 & a_3 \end{bmatrix}. \tag{2}$$

The components a and a_3 describe the derived polarizabilities perpendicular and parallel to the defect axis, respectively. The difference between a and a_3 indicates the anisotropy of the vibrational modes and is reflected in the r/q ratio (Fig. 4 and Table II). The 28-cm^{-1} mode is extremely anisotropic: its r/q ratio is equal to zero, which means that only the polarizability *parallel* to the defect axis is modulated by this dynamical mode. This feature is related to the fact that the 28-cm^{-1} signal is only observed under F_{A1} excitation, which connects the s-like ground state and the p_z excited state. The three modes at 97, 106, and 119 cm^{-1} and the Li^+ mode at 227 cm^{-1} possess a nonzero r/q ratio, establishing a vibronic coupling with *all* the p functions in the excited state.

(ii) In Figs. 3 and 4 and in Table II it is shown that the r/q ratio is strongly frequency dependent. This is reflected in the relative intensities of the $\langle 110\rangle\langle 110\rangle$ and $\langle 1\bar{1}0\rangle\langle 110\rangle$ spectra. Apart from the mode at 28 cm^{-1}, the $F_A(Li^+)$ modes in KBr are characterized by a negative r/q ratio under F_{A1} excitation. In contrast, the 568-nm spectrum exhibits $F_A(Li^+)$ vibrations with r/q values about unity.

(iii) The negative sign of r/q implies that the components a and a_3 are opposite in sign: the vibrational modes, which couple to the F_{A1} transition, modulate the polarizabilities parallel and perpendicular to the defect axis in the opposite way. In this sense the $F_A(Li^+)$ centers in KCl and KBr behave very differently, stimulating further investigations in other host lattices such as RbCl and NaCl.

(iv) Although the experimental accuracy of the polarized spectra under 568-nm excitation can certainly be enhanced by a more complete F- to F_A-center conversion, it is established that the $F_A(Li^+)$ modes possess r/q values which are definitely positive (Table II). In particular, the r/q ratio of the 227-cm^{-1} mode is very close to unity. The relation r/q equal to 1 reflects the fact that the components a and a_3 of the derived polarizability tensor (2) are equal, i.e., the observed form of the Raman tensor corresponds to the A_{1g} representation of the cubic group O_h. Therefore, the polarized Raman properties of the $F_A(Li^+)$ modes under F_{A2} resonant excitation hardly reflect the noncubic symmetry of the $F_A(Li^+)$ center. This is very peculiar for the 227-cm^{-1} mode, since it strongly involves the Li^+ coordinate. In contrast, selecting a laser line in the low-frequency tail of the F_{A1} band reveals the anisotropic character of the $F_A(Li^+)$ center through the much-smaller-than-unity magnitude of the r/q values. The decreasing r/q ratio from 647- to 676-nm excitation (Table II) demonstrates the increasing F_{A1} contribution to the polarized Raman spectra. The 28-cm^{-1} mode is the most anisotropic one. Surprisingly, the motion of the Li^+ ion is hardly involved in this mode, as is reflected in the absence of an isotope shift upon $^7Li^+$-to-$^6Li^+$ substitution (Fig. 2). The nature of this 28-cm^{-1} mode and the similar 47-cm^{-1} mode of the $F_A(Li^+)$ center in KCl are not yet understood.

Finally, we readdress the question of the observability of E-like modes in resonant Raman scattering.[21] For the $F_A(Li^+)$ center in KCl only totally symmetric modes have been identified.[11–14] The two high-frequency modes reflect the motion of the Li^+ ion within the mirror plane.[14] The unidentified mode at 245 cm^{-1} in KCl:$^7Li^+$ (Ref. 13) can be tentatively associated with the Li^+ motion out of the mirror plane. However, due to the small overlap of the F_{A1} and F_{A2} bands in KCl (see Appendix), resonant enhancement of this mode is unlikely.[14,21] In KBr, excitation in the spectral region of overlapping F_{A1} and F_{A2} bands may result in SRE of such E-like modes, since they mix up the three p states of the F_A center and, consequently, the σ and π character of the F_{A1} and F_{A2} bands, respectively.

C. The KBr:Li^+ low-frequency modes: Anharmonic effects

Sievers and Takeno have observed the low-frequency ir-active mode at 16.3 cm^{-1} in KBr:$^7Li^+$. This very small vibrational energy is explained by a drastic reduction of the force constant between the Li^+ impurity ion and its Br^- neighbors, namely to 0.6% of the value in the pure KBr lattice. The isotope shift to 17.9 cm^{-1}, which is larger than the shift for an Einstein oscillator, was assumed to be due to a strong quartic contribution to the potential experienced by the Li^+ ion.[8]

The low-frequency Raman modes at 27 and 37 cm^{-1} exhibit a normal (positive) isotope effect. However, the motion of the Li^+ ion itself cannot be involved in these even-parity Raman modes. The mean Raman shift of these modes exactly coincides with the overtone ir frequency of 32 cm^{-1}. Therefore, in agreement with Ref. 2, we interpret the Raman vibrations as the first overtones of the ir mode. They should belong to one of the representations of the cubic group O_h contained in the product

$T_{1u} \times T_{1u} = A_{1g} + E_g + T_{1g} + T_{2g}$. The difference in vibrational energy between the observed Raman peaks and the exact double ir frequency, as well as the isotope effects and the linewidths, require a detailed reconsideration of the defect potential.

The absence of the T_{2g} contribution in the Raman spectrum is an unsolved problem. At this point it is interesting to compare the KBr:Li^+ data to the Raman spectra of the H_s^- center, which were measured in KI and KBr,[22] and also in KCl.[23] The H_s^- center is a substitutional negative hydrogen ion on an anion site. It possesses an ir mode at 500 cm^{-1} with Raman-active overtones at about 1000 cm^{-1} belonging to the T_{2g}, E_g, and A_{1g} representations.[22,23] For this defect the T_{2g} overtone is the most intense one. A theoretical explanation for this observation is not yet available.[22]

The strongly anharmonic potential, initially proposed to explain the large isotope effect of the low-frequency resonance,[8] could not explain the small electric-field-induced frequency shift of the latter. A static harmonic potential, with an incipient Gaussian barrier lower than the zero-point energy of the Li^+ oscillation, was found to explain both the isotope shift and the Stark effect.[24,25] However, this way one cannot explain the peak positions of the first and second overtones[2] observed in the Raman and ir spectra, respectively. A static potential suitable to describe these peak positions should be much more anharmonic for large vibrational amplitudes.

Sievers and co-workers investigated the isotope effect of the ir resonant modes of KBr:Li^+ and other lattice-impurity systems.[26] Two anharmonic effects were considered: (i) A fourth-order static perturbation, and (ii) coupling with a continuum of (perturbed) lattice modes. Starting from this theoretical work, one can tentatively associate the large isotope shift of the fundamental mode with the *static* anharmonicity of the defect potential. The smaller size of the isotope effect for the Raman-active overtones probably parallels a stronger coupling (dynamic anharmonicity) with the lattice modes. Consistent with this idea are the still smaller isotope effect for the 43-cm^{-1} ir mode of KBr:$^7Li^+$ and the interpretation of this mode as the second overtone of the 16.3-cm^{-1} vibration.

D. Strongly perturbed Li^+ potential

1. The Li^+-perturbed lattice mode at 28 cm^{-1}

The 28-cm^{-1} mode of F_A (Li^+) in KBr:Li^+ is coupled exclusively to the F_{A1} transition. It does not influence the energy difference between the *s*-like ground state and the p_x and p_y levels of the excited state. The fact that this vibration hardly involves the Li^+ coordinate, as is reflected in the zero isotope shift, seems in contradiction with the preferential coupling to the F_{A1} transition.

In KBr there is no correspondence at all between this Raman mode and the low-frequency ir vibration at about 17 cm^{-1} of isolated Li^+. In the KCl:Li^+ system, the low-frequency Raman mode at 43 cm^{-1} is also ir active, because of the off-center position of Li^+. The anomalous isotope shift of the KCl:Li^+ mode probably has to do with its coupling to the tunneling motion of the Li^+ ion.[19] From this point of view, no isotope shift should be expected for the 28-cm^{-1} mode of $F_A(Li^+)$ in KBr, since the Li^+ ion in this system does not exhibit a tunneling motion.

In KBr:Li^+ the on-center position of Li^+, or equivalently the conservation of cubic symmetry, implies the separation of dynamical modes of different parity into the Raman and ir spectra. In this sense the absence of a low-frequency ir mode similar to the 28-cm^{-1} Raman mode supports the idea that the Li^+ ion in KBr:$F_A(Li^+)$ is located on center. It should still be explained why such a low-frequency mode is *not* observed for the *isolated* Li^+ ion in KBr. The *F* center adjacent to the Li^+ ion could enhance the polarizability. For the $F_A(Li^+)$ center in KCl this phenomenon leads to the observability of the high-frequency Li^+ modes, which are not detected for the isolated Li^+ center. The observation of the 47-cm^{-1} Raman mode in KCl:Li^+ and the absence of a similar mode in KBr:Li^+ indicates a larger derived polarizability in KCl:Li^+ than in KBr:Li^+.

2. The Li^+ vibration at 227 cm^{-1}

The 227-cm^{-1} mode of $F_A(^7Li^+)$ in KBr is associated with the $^7Li^+$-ion motion because of its normal isotope shift. In this sense the 227-cm^{-1} mode is related to the T_{1u} mode, i.e., the vibration of the Li^+ impurity itself, which is observed in the ir spectrum of isolated Li^+ at 16.3 cm^{-1}. Therefore, the potential felt by the isolated Li^+ center in KBr is drastically steepened by replacing one Br^- ion by an electron. This is in qualitative agreement with the picture of the flat anharmonic potential of Li^+ in KBr, such that the Li^+ vibrational wave function is smeared out and actual Li^+ position not well defined. Far-ir measurements under hydrostatic pressure on KCl:Li^+ allow one to estimate the full width at half maximum of the Li^+ wave function in KBr, yielding a value of 1 Å, i.e., about one-third of the lattice constant.[27,28] This large extension of the vibrational wave function of Li^+ in KBr may result in a large sensitivity of the Li^+ dynamics to addition of an extra impurity or defect in its vicinity.

The vibrational energies of the Li^+ motion for the isolated Li^+ and $F_A(Li^+)$ centers in KBr provide one illustration of this idea. Another example is the Li^+-pair center.[1–3] Although the precise structure of this defect is not yet understood, it is sure that the presence of a nearby Li^+ ion yields a completely different potential in which a correlated tunneling motion takes place.[1,2]

Finally, we compare the vibrational energies of the high-frequency modes of the $F_A(Li^+)$ center in some other hosts. For the $^7Li^+$ isotope the motion along the defect axis possesses a Raman shift of 264, 266, and 227 cm^{-1} in NaCl,[29] KCl, and KBr, respectively. In this series the vibrational frequency of 227 cm^{-1} for KBr:$F_A(Li^+)$ seems reasonable. However, the very large shift from 16.3 cm^{-1} for the $^7Li^+$ ir vibration of the isolated defect to 227 cm^{-1} for the C_{4v}:A_1 Raman mode of $F_A(^7Li^+)$ is not yet understood.

V. CONCLUDING REMARKS

The low-frequency ir mode around 17 cm^{-1} of the isolated Li^+ defect in KBr reflects the very weak forces on this on-site impurity ion. The strong anharmonicity of the potential experienced by the Li^+ ion is revealed by the Raman-active first overtones and also by the ir-active second overtones of the 17-cm^{-1} mode. In contrast with KCl:Li^+ no nearly degenerate Raman- and ir-active modes are observed, which indicates the conservation of cubic symmetry, i.e., the on-center position of Li^+ in KBr.

The resonant Raman spectra of $F_A(Li^+)$ in KBr exhibit a low-frequency mode at 28 cm^{-1}, in which the Li^+ coordinate hardly participates, and a 227-cm^{-1} vibration of the $^7Li^+$ ion itself along the $F_A(Li^+)$-center axis. The high energy of the latter in comparison with the 16.3-cm^{-1} ir mode demonstrates that the potential experienced by the Li^+ ion is strongly influenced by the adjacent F center. The high sensitivity of the Li^+ dynamics upon addition of extra defects or impurities in its vicinity undoubtedly has to do with the large extension of the Li^+ vibrational wave function and the fact that its on-center position is not well defined in the flat anharmonic potential.

The polarized Raman spectra of the $F_A(Li^+)$ modes in KBr are consistent with totally symmetric representation of the point group C_{4v}. This is in contrast with KCl:Li^+, for which the depolarized Raman scattering under F_{A2} excitation indicates a lower symmetry, corresponding to the off-center position of the Li^+ ion.

The Raman spectra are a superposition of F_{A1} and F_{A2} scattering. These two contributions possess very different polarization properties, which are more difficult to unravel than in the KCl:Li^+ crystal, because of the stronger overlap of the F_{A1} and F_{A2} transitions in KBr. The F_{A1} spectrum shows that the polarizabilities parallel and perpendicular to the defect axis are modulated the opposite way by the $F_A(Li^+)$ vibrations. This feature is very specific for the $F_A(Li^+)$ center in KBr.

ACKNOWLEDGMENTS

The authors wish to thank E. Goovaerts for critically reading the manuscript, and J. M. Spaeth and G. Baldacchini for supplying some of the crystals. The excellent experimental assistance of A. Bouwen is kindly appreciated. This work was supported by the Geconcerteerde Acties (Ministerie van Wetenschapsbeleid, Belgium), by the National Fund for Scientific Research (Belgium), by the Interuniversitair Instituut voor Kernwetenschappen (IIKW, Belgium), and by the U.S. National Science Foundation (NSF) under Grants No. DMR-81-05332 and No. DMR-87-06416, to all of which the authors are greatly indebted.

APPENDIX

The behavior-type (BT) analysis of the polarized Raman spectra of the $F_A(Li^+)$ center in KBr is considered more in detail. The role of the resonance effect and the optical reorientation of the defects is discussed. Possibilities of a more refined data analysis are indicated.

The polarized Raman intensities are presented in Sec. III B. Apart from the continuum of acoustic- and optical-phonon modes, the $F_A(Li^+)$ vibrations exhibit an s/q ratio equal to zero within experimental accuracy. This means that the off-diagonal components of the Raman tensor can be neglected and, therefore, one does not need the extended BT method for nonsymmetric Raman tensors, as was necessary to study the $F_A(Li^+)$ center in KCl (Ref. 14) and the Tl^+-perturbed $Tl^0(1)$ center in KCl, KBr, and RbCl.[16] From this viewpoint the data of the $F_A(Li^+)$ center in KBr can be treated in the same way as those of the unperturbed $Tl^0(1)$ defect.[21]

In all KCl:Li^+ and in x-irradiated KBr:Li^+ crystals the exciting laser light induces optical reorientation of the $F_A(Li^+)$ center, which results in a nonrandom distribution of the $F_A(Li^+)$ center among its possible orientations.[11–14] Because of a different mechanism, the reorientation of the $F_A(Li^+)$ center in KBr is less efficient than in KCl, but polarized optical-absorption measurements clearly demonstrate the necessity of considering a nonrandom distribution. In this case the r/q ratio introduced in Sec. III B is given by a more general expression:

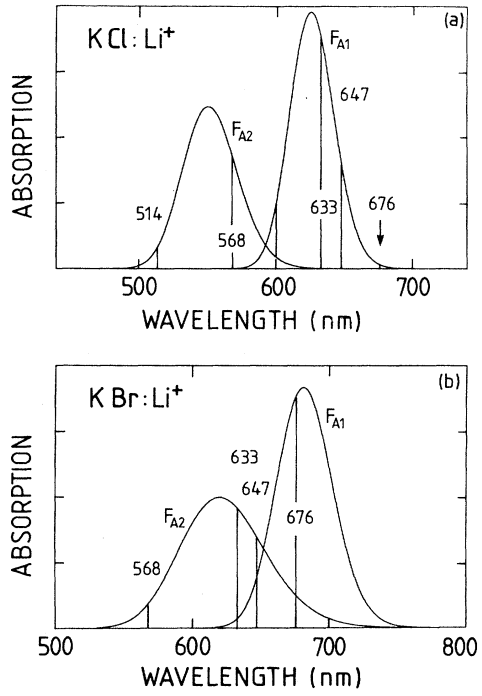

FIG. 5. Approximate Gaussian line shapes are depicted for the F_{A1} and F_{A2} transitions of the $F_A(Li^+)$ center in (a) KCl and (b) KBr taking into account the experimental values for the peak positions and linewidths (from Ref. 12). The integrated absorption is normalized. The wavelengths of some relevant laser lines are also indicated. The overlap of the F_{A1} and F_{A2} bands is much smaller in KCl than in KBr.

$$\frac{r_1}{q_2}=\frac{2N_y a a_3+N_x a^2}{(N_x+N_y)a^2+N_y a_3^2}\ . \tag{A1}$$

Here, a and a_3 denote the diagonal components of the $C_{4v}:A_1$ Raman tensor and N_i are the population numbers of the three possible orientations of the $F_A(Li^+)$ center, as depicted in Fig. 2 of Ref. 14. For the $F_A(Li^+)$ center in KBr under F_{A1} and F_{A2} excitation, N_y and N_z are equal. The ratio r_1/q_2 is frequency dependent through the frequency dependence of a and a_3, and the population numbers. We have calculated the latter for a stationary regime by assuming a Gaussian profile for the F_{A1} and F_{A2} bands (see Fig. 5). Some typical observations for the r_1/q_2 ratio are presented in Table II of Sec. III. Apart from the 28-cm^{-1} mode all the $F_A(Li^+)$ modes possess r_1/q_2 values, which are definitely negative, but still large enough to exclude the $C_{4v}:B_1$ mode, for which the r_1/q_2 value lies between -0.5 and -1.

The variation of the r_1/q_2 ratio from -0.50 to -0.20 by tuning the excitation frequency from 647 to 676 nm reflects the larger contribution of F_{A1} scattering. In x-irradiated KCl:Li^+ we established an s_2/q_2 ratio equal to zero for both the continuum and the localized modes under F_{A1} excitation.[14] The C_{1h} symmetry, which reflects the off-center position of the Li^+ ion in this center, is thus obscured by SRE. However, it should be mentioned that this polarized Raman property was not observed in additively colored samples.[13]

More detailed conclusions beyond the BT analysis can be obtained by taking into account expression (A1). Provided that after a long enough exposure to the laser light, the population numbers N_i of the $F_A(Li^+)$ center are close to the stationary-state values, one can replace N_i in (A1) by the solutions of the rate equations[30] and derive the ratio a/a_3 from the observed r_1/q_2 value. In KBr this allows one to distinguish the A_1 modes according to their anisotropy a/a_3. In KCl the a/a_3 ratio is a function of the off-center tilting angle with respect to the crystal's ⟨100⟩ directions. Consequently, polarized Raman scattering can be considered an independent technique to study this tilting angle through the determination of the r_1/q_2 value.

[1] R. J. Russell and F. Bridges, Phys. Rev. B **26**, 3386 (1982).
[2] L. H. Greene and A. J. Sievers, Phys. Rev. B **31**, 3948 (1985).
[3] E. R. Grannan and J. P. Sethna, Bull. Am. Phys. Soc. **31**, 697 (1986).
[4] R. J. Quigley and T. P. Das, Phys. Rev. **177**, 1340 (1969).
[5] W. D. Wilson, R. D. Hatcher, G. J. Dienes, and R. Smoluchowski, Phys. Rev. **184**, 844 (1969).
[6] C. R. A. Catlow *et al.*, Phys. Rev. B **18**, 2739 (1978).
[7] M. J. L. Sangster, J. Phys. C **13**, 5279 (1980).
[8] A. J. Sievers and S. Takeno, Phys. Rev. **140**, A1030 (1965).
[9] A. Mabud and F. Lüty, Bull. Am. Phys. Soc. **28**, 452 (1983); Abstract Book of the International Conference on Defects in Insulating Crystals (Salt Lake City, 1984), p. 301 (unpublished).
[10] A. Mabud and F. Lüty, Bull. Am. Phys. Soc. **28**, 452 (1983); Abstract Book of the International Conference on Defects in Insulating Crystals (Salt Lake City, 1984), p. 299 (unpublished).
[11] B. Fritz, in *Localized Excitations in Solids,* edited by R. F. Wallis (Plenum, New York, 1968), p. 496.
[12] F. Lüty, in *Physics of Color Centers,* edited by W. B. Fowler (Academic, New York, 1968), p. 181.
[13] D. S. Pan and F. Lüty, in *Proceedings of the Third International Conference on Light Scattering in Solids, Campinas, Brazil, 1975,* edited by M. Balkanski, R. C. C. Leito, and S. P. S. Porto (Flammarion, Paris, 1975), p. 539.
[14] M. Leblans, W. Joosen, E. Goovaerts, and D. Schoemaker, Phys. Rev. B **35**, 2405 (1987).
[15] J. F. Zhou, E. Goovaerts, and D. Schoemaker, Phys. Rev. B **29**, 5509 (1984); **29**, 5533 (1984); E. Goovaerts, J. F. Zhou, W. Joosen, and D. Schoemaker, Cryst. Lattice Defects Amorph. Mater. **12**, 317 (1985).
[16] W. Joosen, E. Goovaerts, and D. Schoemaker, Phys. Rev. B **35**, 8215 (1987).
[17] R. D. Kirby, A. E. Hughes, and A. J. Sievers, Phys. Rev. B **2**, 481 (1970).
[18] W. Joosen, E. Goovaerts, and D. Schoemaker, Phys. Rev. B **34**, 1273 (1986).
[19] M. Van Himbeeck, H. De Raedt, W. Joosen, and D. Schoemaker, Europhys. Lett. **4**, 141 (1987).
[20] M. J. L. Sangster and A. M. Stoneham, Phys. Rev. B **26**, 1028 (1982).
[21] W. Joosen, E. Goovaerts, and D. Schoemaker, Phys. Rev. B **32**, 6748 (1985).
[22] G. P. Montgomery, Jr., W. R. Fenner, M. V. Klein, and T. Timusk, Phys. Rev. B **5**, 3343 (1972).
[23] Y. Kondo, J. R. Duffey, and F. Lüty, Phys. Rev. B **23**, 28 (1981).
[24] B. P. Clayman, R. D. Kirby, and A. J. Sievers, Phys. Rev. B **3**, 1351 (1971).
[25] A. S. Barker, Jr. and A. J. Sievers, Rev. Mod. Phys. Suppl. 2 **47**, 106 (1975).
[26] R. D. Kirby, I. G. Nolt, R. W. Alexander, and A. J. Sievers, Phys. Rev. **168**, 1057 (1968).
[27] A. M. Kahan, M. Patterson, and A. J. Sievers, Phys. Rev. B **14**, 5422 (1976).
[28] R. P. Devaty and A. J. Sievers, Phys. Rev. B **22**, 4074 (1980).
[29] M. Leblans (unpublished).
[30] G. Baldacchini *et al.*, Phys. Rev. B **33**, 4273 (1986).